Stopped-Flow Kinetic Analysis of the Interaction of Anthraquinone Anticancer Drugs with Calf Thymus DNA, Poly[d(G-C)]·Poly[d(G-C)], and Poly[d(A-T)]·Poly[d(A-T)]†

C. R. Krishnamoorthy,‡ Shau-Fong Yen,‡ J. C. Smith,‡ J. William Lown,§ and W. David Wilson*,‡

Department of Chemistry and Laboratory for Microbial and Biochemical Sciences, Georgia State University, Atlanta, Georgia 30303-3083, and Department of Chemistry, University of Alberta, Edmonton, Alberta T6G 2G2, Canada

Received February 25, 1986; Revised Manuscript Received June 6, 1986

ABSTRACT: The sodium dodecyl sulfate driven dissociation reactions of daunorubicin (**1**), mitoxantrone (**2**), ametantrone (**3**), and a related anthraquinone without hydroxyl groups on the ring or side chain (**4**) from calf thymus DNA, poly[d(G-C)]$_2$, and poly[d(A-T)]$_2$ have been investigated by stopped-flow kinetic methods. All four compounds exhibit biphasic dissociation reactions from their DNA complexes. Daunorubicin and mitoxantrone have similar dissociation rate constants that are lower than those for ametantrone and **4**. The effect of temperature and ionic strength on both rate constants for each compound is similar. An analysis of the effects of salt on the two rate constants for daunorubicin and mitoxantrone suggests that both of these compounds bind to DNA through a mechanism that involves formation of an initial outside complex followed by intercalation. The daunorubicin dissociation results from both poly[d(G-C)]$_2$ and poly[d(A-T)]$_2$ can be fitted with a single exponential function, and the rate constants are quite close. The ametantrone and **4** polymer dissociation results can also be fitted with single exponential curves, but with these compounds the dissociation rate constants for the poly[d(G-C)]$_2$ complexes are approximately 10 times lower than for the poly[d(A-T)]$_2$ complexes. Mitoxantrone also has a much slower dissociation rate from poly[d(G-C)]$_2$ than from poly[d(A-T)]$_2$, but its dissociation from both polymers exhibits biphasic kinetics. Possible reasons for the biphasic behavior with the polymers, which is unique to mitoxantrone, are selective binding and dissociation from the alternating polymer intercalation sites and/or dual binding modes of the intercalator with both side chains in the same groove or with one side chain in each groove.

A large number of DNA[1]–intercalator binding studies have been conducted, but there have been far fewer studies of the dynamics of the interactions. With their extensive analysis of the kinetics of the interaction of actinomycin analogues with DNA, Müller and Crothers (1968) clearly established the necessity of this type of investigation in developing an understanding of DNA intercalation complexes. In addition, they established a potential link between the intercalation kinetics and the biological effects of the compound as an anticancer drug. The basic idea is that to be active a compound must have both strong binding to DNA and slow dissociation kinetics. Either of these alone would be insufficient to block polymerase activities in target cells.

Although the kinetics of dissociation of only a few intercalator–DNA complexes have been analyzed in detail, the following general order of dissociation rate constants exists: acridines (Li & Crothers, 1969; Dourlent & Hogrel, 1976; Ramstein et al., 1976; Marcandalli et al., 1984) > phenanthridines (Mandal et al., 1980; Ryan & Crothers, 1984; Wilson et al., 1985; Chandrasekaran et al., 1984; Macgregor et al., 1985) > anthracyclines (Wilson et al., 1976; Chaires et al., 1985; Fox et al., 1985) > actinomycin (Müller & Crothers, 1968; Shafer et al., 1980; Fox & Waring, 1984), nogalamycin (Fox et al., 1985). This is only a crude comparison since most of these compounds exhibit complex rate processes with DNA and can have significant base-pair-dependent interaction rates.

Mitoxantrone type anthraquinone antitumor drugs (Murdock et al., 1979) are interesting from several standpoints: (1) they have shown excellent clinical anticancer activity (Rozencweig et al., 1983); (2) they have a similar activity spectrum but less severe cardiotoxic effects than anthracyclines (Rozencweig et al., 1983); (3) they cause large changes in chromatin structure (Citarella et al., 1982); (4) as a consequence of the positioning of their two cationic substituent chains, they can have two distinct types of binding modes with both side chains in one groove or one side chain in each groove (Islam et al., 1985; Balaji et al., 1985; Lown et al., 1985; Lown & Hanstock, 1985). There is strong evidence that the interaction of mitoxantrone with cellular DNA contributes significantly to its specific cytotoxic action (Lown et al., 1984, 1985). The molecular relationship of structural changes in mitoxantrone derivatives to changes in DNA interactions and effects on activity are not known. We have recently investigated the mode of binding, binding strength, and binding specificity for mitoxantrone and a series of related derivatives (Lown et al., 1985). As might be expected from their structure, these compounds bind to DNA by intercalation. They show binding selectivity for G/C base pairs, but structural variations have significant effects on binding strength. Mitoxantrone, for example, with two hydroxyl groups on the substituted anthraquinone ring system, has a binding constant similar to that

† This research was supported by grants from the NIH (GM 30267 to W.D.W.) and the National Cancer Institute of Canada (to J.W.L.) and by a contract between J.W.L. and the National Foundation of Cancer Research.

‡ Georgia State University.
§ University of Alberta.

[1] Abbreviations: DNA, deoxyribonucleic acid; PIPES, piperazine-*N*,*N*′-bis(2-ethanesulfonic acid); poly[d(A-T)]$_2$, poly[d(A-T)]·poly[d(A-T)]; poly[d(G-C)]$_2$, poly[d(G-C)]·poly[d(G-C)]; SDS, sodium dodecyl sulfate; EDTA, ethylenediaminetetraacetic acid; 2D, two dimensional; NMR, nuclear magnetic resonance; NOE, nuclear Overhauser effect; SSR, sum of the squared residuals.

0006-2960/86/0425-5933$01.50/0

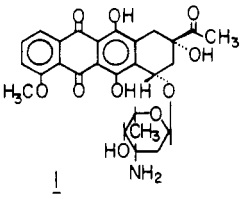

1

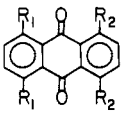

2 R_1 = OH
R_2 = $NHCH_2CH_2NHCH_2CH_2OH$

3 R_1 = H
R_2 = $NHCH_2CH_2NHCH_2CH_2OH$

4 R_1 = H
R_2 = $NHCH_2CH_2N(CH_3)_2$

FIGURE 1: Structures for daunorubicin (**1**), mitoxantrone (**2**), ametantrone (**3**), and **4**.

of daunorubicin, but binds to DNA more strongly than ametantrone, which does not have the ring hydroxyl groups (Lown et al., 1985).

Müller and Crothers (1968) demonstrated with actinomycin that dissociation of drugs from DNA could be driven with SDS and measured by stopped-flow techniques. As indicated above, they also suggested that dissociation rate constants might be as important in evaluating activity as thermodynamic comparisons, and it is essential to evaluate dissociation reactions for drugs of known activity to test this idea. In addition, a complete understanding of the molecular aspects of the interactions of mitoxantrone and related compounds with DNA requires both kinetic and thermodynamic analyses as well as studies by spectroscopic and X-ray methods. We describe here the effects of drug structure, temperature, ionic strength, and DNA base-pair composition on the SDS-driven dissociation of mitoxantrone, ametantrone, and **4** from DNA (structures in Figure 1). The ionic strength analysis was found to be particularly useful in distinguishing among possible mechanistic pathways for drug–DNA interactions. We have conducted similar experiments with daunorubicin (**1**) for comparative purposes. Limited association kinetics results are also presented.

Materials and Methods

Compounds. Mitoxantrone, ametantrone, and **4** (Figure 1) were supplied by Dr. K. C. Murdock of Lederle Laboratories, Pearl River, NY. Their synthesis, purification, and properties have been described previously (Murdock et al., 1979). Daunorubicin was purchased from Boehringer-Mannheim and was found to be pure by thin-layer chromatography (TLC) and NMR and UV–visible spectral analysis.

Buffers. PIPES buffers contained 10 mM PIPES, 1 mM EDTA, and sodium chloride as follows: PIPES 10, 0.1 M NaCl; PIPES 20, 0.2 M NaCl; PIPES 50, 0.5 M NaCl. All were adjusted to pH 7.0.

DNA Samples. Calf thymus DNA from Worthington and polymers from P-L Biochemicals were prepared as previously described (Wilson et al., 1985).

Kinetics. Kinetic measurements were made by using an Aminco-Morrow stopped-flow apparatus adapted to a Johnson Foundation MB2 air turbine spectrophotometer. The output from the instrument was fed to an Olis 3820 data-acquisition system for storage on magnetic disk and subsequent analysis. Typically, several runs were stored and averaged before final analysis. Two hundred data points in a preselected time range could be fitted by using from one to three exponential curves. Fitting was done with software supplied with the Olis system and with a program based on the Marquardt–Levenberg algorithm (written and generously given to us by Professor R. H. Shafer, Department of Pharmaceutical Chemistry, University of California, San Francisco). Dissociation experiments were conducted by mixing equal volumes (100 μL) of an intercalator–DNA complex and a 1.0% sodium dodecyl sulfate solution. Daul-wavelength difference spectra were obtained as a function of time by using the wavelength pair 450 and 580 nm for **4**, 469 and 550 nm for daunorubicin, and 469 and 612 nm for mitoxantrone and ametantrone. Data collection was begun 5 ms after initiation of mixing, and the instrument response time constant was set at 2 ms. At the gain settings used in these experiments, the voltage-to-absorbance conversion factor on the attached traces is 0.01 absorbance units to 100 mV. The zero-voltage balance setting was typically set near the value for the dissociated intercalator. Association kinetics measurements were conducted under pseudo-first-order conditions in a similar manner. Equal volumes (100 μL) of a DNA solution and a solution of the intercalator were mixed under the desired conditions and data collected as above. Typically, five to eight runs of this type were averaged in the computer to improve the signal-to-noise ratio.

Results

Dissociation from DNA: Effect of Intercalator Structure. Results for the SDS-driven dissociation of daunorubicin from calf thymus DNA are shown in Figure 2. The results for fitting the data with both single and dual exponential functions are also shown in the figure. As an operational approach to deciding the minimum number of exponentials to use in fitting multiphasic kinetic curves, we analyze the minimized sum of the squared residuals (SSR) and add exponentials until this sum does not change significantly relative to the experimental random error in the dependent variable, the amplitude in these kinetics experiments. We then analyze a plot of the residuals in the amplitude vs. time and again reject the fit if there is any significant systematic trend in the residuals (Turner et al., 1981). For the daunorubicin results in Figure 2, there is a systematic trend in the residuals in the one-exponential fit but not in the two-exponential fit. The SSR improves from 35×10^{-4} to 7.2×10^{-4} in going from the one- to the two-exponential fit. The SSR, however, only changes to 7.0×10^{-4} in going to a three-exponential fit and the distribution of residuals is not significantly changed (relative to the random noise). We therefore reject the one-exponential fit because it is not satisfactory to explain the kinetics. Also, the three-exponential fit is rejected in favor of the two-exponential fit shown in Figure 2 because addition of the third exponential does not significantly improve the fit. A similar approach has been used to analyze all kinetic results in this paper. The correlation coefficient for the fit, as expected (Turner et al., 1981), is fairly uniformative in deciding among one-, two-, and three-exponential fits to the data. Results for the dual exponential fit are shown in Table I. The errors in the rate constants will obviously depend on the signal to noise for the plot, the total amplitude how many exponentials are required to fit the curves, etc. For the results in this paper, such as those shown in Figure 2, the rate constants are fit to ±10% with the 90% confidence limit.

DNA contains 10 dinucleotide intercalation sites (Waring, 1981) for molecules such as those shown in Figure 1, and rates

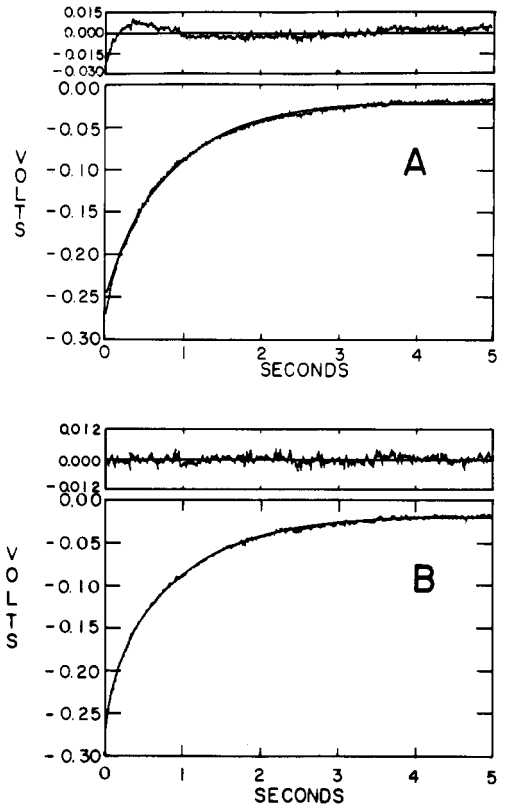

FIGURE 2: SDS-driven dissociation reactions at 20 °C in PIPES 10 buffer for a daunorubicin–DNA complex at a ratio of 1:10 daunorubicin:DNA base pairs. A total of 200 data points were collected in the specified time span, and the points were consecutively connected. Smooth lines in panel A and panel B are (1)- and (2)-exponential nonlinear least-squares best fit values to the experimental data, respectively. Above each experimental plot the corresponding residual plots for the fits are shown. The plots are photomultiplier voltages (or for residual plots voltage differences) as a function of time.

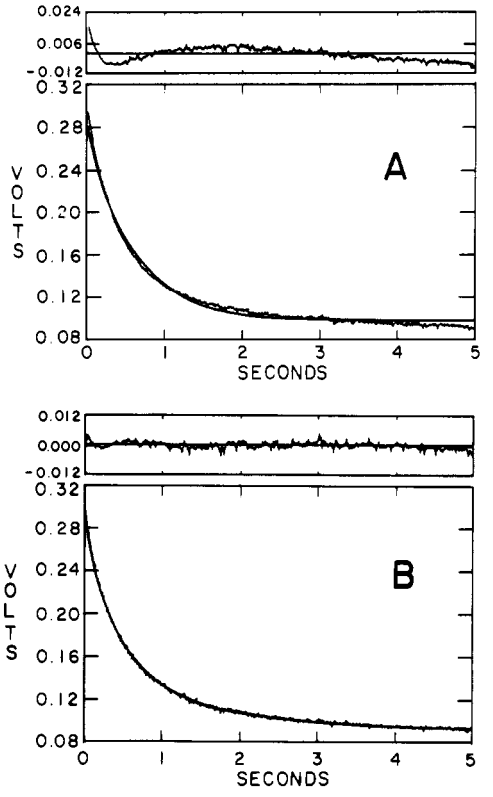

FIGURE 3: SDS-driven stopped-flow dissociation reactions at 20 °C in PIPES 10 buffer for a DNA–mitoxantrone complex. The DNA concentration in base pairs is 5×10^{-5} M, which is 10 times the concentration of mitoxantrone. A total of 200 data points were collected and plotted as in Figure 2. The smooth line in panel A represents the single-exponential nonlinear least-squares best fit values for the experimental data, and panel B is a two-exponential fit for the same data. Residual plots for both data sets are shown above the experimental plots.

Table I: Dissociation Kinetics Results for Complexes of **1–4** with DNA[a]

compound	k_1 (s^{-1})	% A^b	k_2 (s^{-1})	% A^b	app half-life (s)
daunorubicin (**1**)	0.97	69	4.4	31	0.4
mitoxantrone (**2**)	0.82	40	3.5	60	0.3
ametantrone (**3**)	2.7	44	17	56	0.1
4	2.9	20	19	80	0.05

[a] Experiments in PIPES 10 buffer at 20 °C with a ratio of intercalator to DNA base pairs of 10 and a DNA base pair molarity of 5×10^{-5}. [b] The amplitude of each phase is given as a percent of the total amplitude.

of association and dissociation with each site could be different. To resolve the different possible kinetic constants from a relatively smooth kinetics curve of, for example, absorbance vs. time typically involves some type of computerized nonlinear fitting routine (Turner et al., 1981) as shown in Figure 2. A single-exponential fit requires obtaining best fit values for up to three parameters—the rate constant, amplitude, and base line position. A two-exponential fit requires up to five parameters due to the addition of another rate constant and amplitude. With multiple rate constants and amplitudes, there is some correlation in the fit values and their resolution will depend on how well separated the two rates are. For all results a window is created where compensating changes in rate constants and amplitudes give essentially the same quality of fit, and the size of the window depends on how highly correlated the parameters are and on other factors such as the presence of systematic error in the experiments. This is more of a problem in fitting kinetic results than, for example, spectral curves due to the inherently low resolution of rate plots. The dual rates shown for daunorubicin–DNA dissociation in Figure 2, thus, probably represent two families of rates with several components in each which are too similar to be resolved. Reactions of low amplitude that have different rate constants also would not be easily resolved even though they do not fall into one of the two groups. On the basis of the known extinction coefficients of daunorubicin free and bound to DNA, however, no significant amount of amplitude could be escaping detection in the experiment, and the two rates shown in Figure 2 give an accurate representation of the major dissociation processes which exist for daunorubicin–DNA complexes. Chaires et al. (1985) and Fox et al. (1985) have also resolved the dissociation reaction of the daunorubicin–DNA complex into two exponentials, and their results, were comparable, are in excellent agreement with those of Table I.

Dissociation experiments for mitoxantrone–DNA complexes were conducted as with daunorubicin, and one set of results, under the same conditions as with daunorubicin in Figure 2, is shown as an example in Figure 3. Results for a single-exponential fit are shown in Figure 3A and those for a dual-exponential fit in Figure 3B. As with daunorubicin, a significant improvement in both the SSR and distribution of residuals is obtained in going from the single- to the dual-exponential fit and the results for the two exponential fits are shown in Table I. Also as with daunorubicin, no significant improvement in SSR was obtained in going to a three-exponential fit (SSR: one exponential, 166×10^{-4}; two exponen-

tials, 9.0×10^{-4}; three exponentials, 5.0×10^{-4}). Again we expect that the two best fit rate processes actually represent families of rates, at different intercalation sites, which can not be resolved under our conditions. Decreasing the ratio of base pairs per mitoxantrone from 10 to 5 did not cause a significant change in the rate constants or amplitudes for the dissociation of mitoxantrone–DNA complexes under the conditions of Figure 3. Denny and Wakelin (manuscript in preparation) have recently completed an analysis of the SDS-driven dissociation of **2**–**4** from DNA (personal communication). Using a dual time based collection with 500 data points and a curve-stripping method of data analysis, they fitted dissociation kinetics curves of **2**–**4** to a sum of three exponential functions. In every case, if the two closer values of their rate constants are averaged for common compounds, their results are quite close to ours for both rate constants and amplitudes. As stated above, there may actually be up to 10 different dissociation rate constants for the 10 different dinucleotide intercalation sites in DNA, which resolve into two major group types whose general characteristics are shown in Table I.

It is interesting to compare qualitatively an apparent half-life, the time for half of the total absorbance change to occur, for the daunorubicin and mitoxantrone dissociation reactions in Figures 2 and 3, respectively. This apparent half-life is approximately 0.4 s for daunorubicin and 0.3 s for mitoxantrone. If the rates from Table I are compared, it can be seen that mitoxantrone has lower rate constants for both the fast and slow phases of the dissociation reaction but still has a shorter apparent half-life than daunorubicin. This apparent inconsistency is explained by analysis of the amplitudes of the two phases. With daunorubicin the slow phase accounts for greater than 60% of the absorbance change while for mitoxantrone the fast phase is responsible for approximately 60% of the change in absorbance. On the whole, these offsetting factors result in two complex dissociation curves that are actually quite similar. Dissociation experiments, carried out under the same conditions as in Figures 2 and 3, for DNA complexes of amentantrone and **4** also required a dual exponential function for fitting and did not improve, within experimental error, in going to a three-exponential fit. The results for all four compounds are collected in Table I. Both amentantrone and **4** have larger rate constants for both the fast and slow dissociation phases than daunorubicin and mitoxantrone. Daunorubicin has the largest amplitude for the slow phase, mitoxantrone and ametantrone have similar amplitudes for both phases and **4** has the smallest amplitude for the slow phase and, thus, the shortest apparent half-life for dissociation.

Dissociation from DNA: Effect of Temperature and Drug Structure. Experiments such as those shown in Figures 2 and 3 were repeated at several temperatures for daunorubicin, mitoxantrone, and ametantrone. The temperatures that can be covered in this type of experiment are limited (by measurable rates at high temperature and instrumentation limits at low temperature), and activation energies for the three compounds, determined from the slopes of linear Arrhenius plots (14–16 kcal/mol), can not be distinguished outside of experimental error. Even over this range, however, some general trends are obvious: (1) mitoxantrone has the lowest and ametantrone the highest dissociation rate constants over this temperature range; (2) as a general trend, dissociation activation energies are similar for mitoxantrone and daunorubicin and are lower for ametantrone; (3) the effect of temperature on the fast and slow reaction phases is similar for all three compounds. With **4** the rate becomes too fast to measure accurately with our instrument as the temperature is increased above 20 °C.

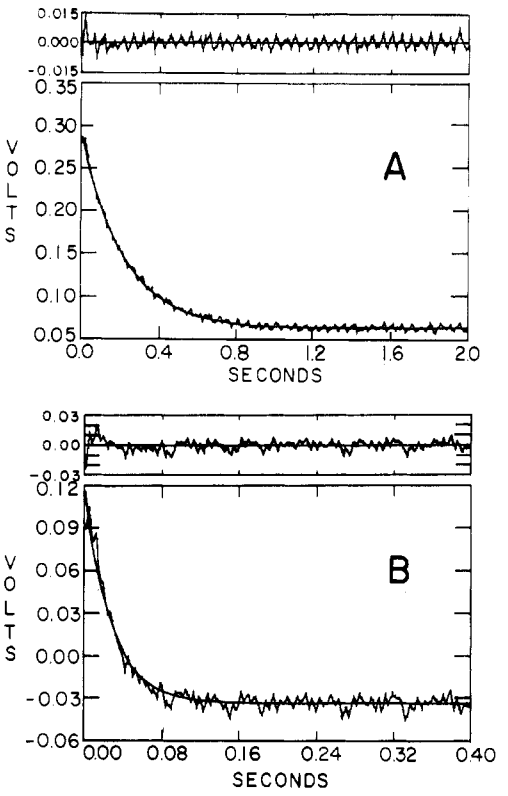

FIGURE 4: SDS-driven dissociation reaction for the **4**–polymer complexes at 20 °C in PIPES 10 buffer. A total of 200 data points were collected and plotted as in Figure 2. Smooth lines in both panels represent the single-exponential nonlinear least-squares best fit values for the poly[d(G-C)$_2$] (A) and poly[d(A-T)]$_2$ (B) complexes. Corresponding residual plots are shown for both data sets.

Dissociation from DNA Polymers: Effect of Temperature and Drug Structure. By the use of the same conditions and methods as described for natural DNA, the SDS-driven dissociation of **1**–**4** from the alternating polymers poly[d(A-T)]$_2$ and poly[d(G-C)]$_2$ was investigated. Dissociation of daunorubicin, ametantrone, and **4** from both polymers could all be fitted to single-exponential curves by using the criteria described above. The results for dissociation of mitoxantrone from both polymers required dual-exponential fits. Daunorubicin has very similar dissociation constants from both polymers but mitoxantrone, ametantrone, and **4** dissociate much more slowly from poly[d(G-C)]$_2$ than from poly[d(A-T)]$_2$. Dissociation curves of **4** with the polymers are shown in Figure 4 and a similar experiment with poly[d(G-C)]$_2$ is shown for mitoxantrone in Figure 5 to illustrate the single- and dual-exponential functions required to fit the results for **4** and mitoxantrone, respectively. Similar dissociation experiments were conducted for the complexes of **1**–**4** with the two polymers as a function of temperature, and the single-exponential best fit rate constants for **1**, **3**, and **4** are shown in Arrhenius plot in Figure 6. As can be seen, the dissociation constants for duanorubicin from the two polymers are similar, the plots for both polymers have very similar slopes, and the activation energy for daunorubicin dissociation from both polymers is 17 ± 1 kcal/mol. Over the temperature range that could be covered, the dissociation of daunorubicin from poly[d(A-T)]$_2$ is always slightly faster than that for poly[d(G-C)]$_2$ (at 20 °C, for example, the dissociation constants are 2.3 s^{-1} for poly[d(G-C)$_2$] and 3.0 s^{-1} for poly[d(A-T)]$_2$). A similar ratio of dissociation constants, at a single temperature, was seen for daunorubicin with these polymers by Fox et al.

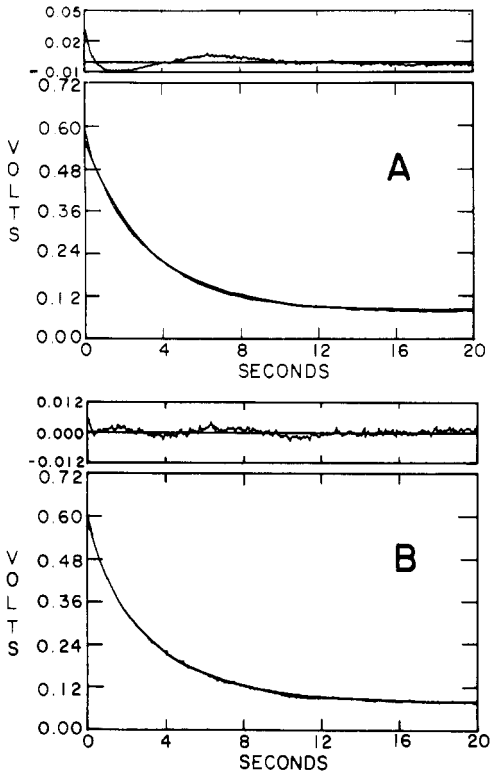

FIGURE 5: Stopped-flow dissociation reactions at 20 °C in PIPES 10 buffer for poly[d(G-C)]$_2$–mitoxantrone at a ratio of 1:10 mitoxantrone:polymer base pairs. A total of 200 data points were collected over a period of 20 s. The smooth line in panel A represents single-exponential nonlinear least-squares best fit values, and panel B is the dual-exponential fit for the same experimental data. The residual plots for each data set are shown above the experimental plots.

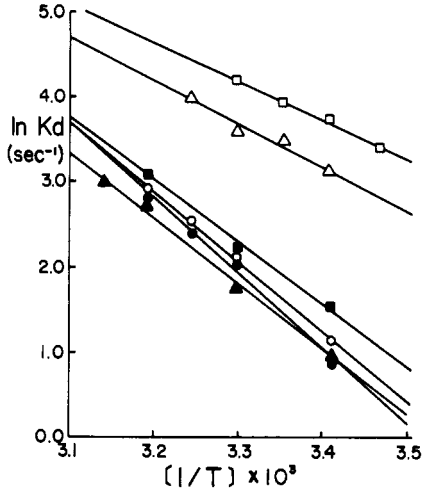

FIGURE 6: Arrhenius plot for SDS-driven dissociation of daunorubicin (**1**) (●, ○), ametantrone (**3**) (▲, △), and **4** (■, □) from poly[d(G-C)]$_2$ (closed symbols) and poly[d(A-T)]$_2$ (open symbols). Experiments were conducted as a function of temperature and were analyzed as shown in Figure 4.

(1985). Over the temperature range in Figure 6, the dissociation of amentantrone and **4** from poly[d(G-C)]$_2$ is significantly slower than from poly[d(A-T)]$_2$. For the individual polymers ametantrone always dissociates more slowly than **4**. Dissociation rate constants for ametantrone and daunorubicin with poly[d(G-C)]$_2$ are similar but the daunorubicin dissociation constant for poly[d(A-T)]$_2$ is much lower than for ametantrone from the same polymer. Approximate activation energies calculated from the plots (Figure 6) are 16 and 11 kcal/mol for dissociation of ametantrone from poly[d(G-C)]$_2$ and poly[d(A-T)]$_2$, respectively, and 14 and 9 kcal/mol for

Table II: Comparison of DNA and Polymer Dissociation Results for Mitoxantrone[a]

type of DNA	k_1 (s^{-1})	% A^b	k_2 (s^{-1})	% A^b
calf thymus	0.82	40	3.5	60
poly[d(G-C)]$_2$	0.29	83	1.3	17
poly[d(A-T)]$_2$	3.0	65	9.3	35

[a] Experiments in PIPES 10 buffer at 20 °C with a ratio of intercalator to DNA base pairs of 10. [b] The amplitude of each phase is given as a percent of the total amplitude.

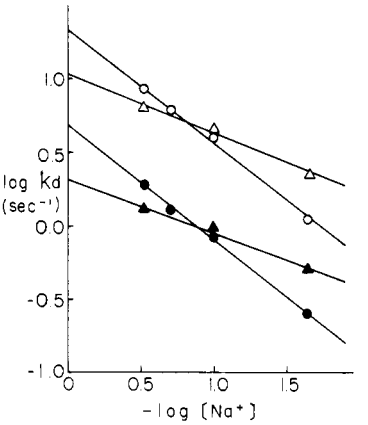

FIGURE 7: Plots of log k_d vs. –log [Na^+] for daunorubicin (▲, △) and mitoxantrone (●, ○) complexes with CTDNA. The kinetic measurements were made at 20 °C in PIPES buffer at various sodium ion concentrations. The DNA concentration in base pairs was kept at 5×10^{-5} M and is 10 times the concentration of mitoxantrone and daunorubicin. Rate constants were calculated from a two-exponential fit to the dissociation decay curves as indicated in Figures 2 and 3. The slow-phase rate constants for both compounds are plotted as closed symbols and the fast-phase rate constants as open symbols.

dissociation of **4** from the same polymers. The dissociation rates for **4** with poly[d(A-T)]$_2$ were too high above 30 °C to obtain accurate kinetic constants.

As illustrated in Figure 5, dissociation of mitoxantrone from both poly[d(G-C)]$_2$ and poly[d(A-T)]$_2$ requires the sum of two exponential functions to fit the observed plots of absorbance vs. time. A comparison of the dissociation constants for mitoxantrone from calf thymus DNA and the two polymers at 20 °C is presented in Table II. The dissociation reactions of mitoxantrone from the polymers were also followed at different temperatures. Both dissociation rate constants for the mitoxantrone–poly[d(G-C)]$_2$ complex are lower than the two rate constants for the poly[d(A-T)]$_2$ complex, and temperature effects on all rate constants are similar.

Dissociation from DNA: Effect of Salt. Experiments such as those shown in Figures 2 and 3 were conducted at constant temperature as a function of salt concentration, and log k_d is plotted vs. –log [Na^+] for these results in Figure 7. For mitoxantrone the linear least-squares slopes for both lines are 0.8 ± 0.03, and for daunorubicin both slopes fall in the range 0.4 ± 0.03, which is in good agreement with theoretical predictions for di- and monocationic intercalators dissociating from the DNA double helix (Wilson et al., 1985). The amplitudes for the fast and slow reaction phases are relatively insensitive to the salt concentration and remain near 70%/30% for the slow and fast phases for daunorubicin and approximately 40%/60% for mitoxantrone as in Figures 2 and 3. It is interesting to note that both rates for mitoxantrone are lower than the daunorubicin rates at low salt concentration but are larger than the daunorubicin rates at salt concentrations of approximately 0.2 M and above.

Association with DNA. As expected from previous studies and theoretical predictions, all compounds associate with DNA

very rapidly at low salt concentration and the rates are outside of the range of our instrument. At high salt concentrations where the rates could be measured, spectral results indicate that mitoxantrone and ametantrone are extensively dimerized in solution, and as a result, the amplitudes for association are too small for accurate measurements. We have, therefore, been unable to obtain reliable association results for **2**–**4**. Association results for daunorubicin with calf thymus DNA have been reported (Chaires et al., 1985). Association of daunorubicin with poly[d(A-T)]$_2$ and poly[d(G-C)]$_2$ at 20 °C in PIPES 10 buffer under pseudo-first-order conditions gave rate constants of 54 and 15 s^{-1}, respectively. The polymer concentration in base pairs in these experiments was 1.25×10^{-5} M, and at higher concentrations the reactions become too fast to measure with our instrument.

Discussion

In a stopped-flow kinetics analysis of the interaction of propidium and ethidium with DNA, we have found that for these compounds the basic mechanism of binding consists of two steps (Wilson et al., 1985). A fast step, which could not be directly detected by stopped-flow methods but which was apparent in analysis of ionic strength effects on the kinetics, was assigned to initial condensation type ionic interaction of the intercalators with the anionic DNA backbone. This was then followed by the observed insertion of the intercalator ring system between base pairs. Although only one rate could be resolved in this process of insertion of the phenanthridium ring into the 10 potential dinucleotide intercalation sites (Waring, 1981), as described above, this probably actually represents a family of rates which cannot be distinguished within our experimental error. Jovin and Striker (1977) using fluorescence detected *T*-jump methods, MacGregor et al. (1985) using pressure-jump methods, and Madal et al. (1980) using stopped-flow methods have found similar results for ethidium. Proflavin seems to bind to DNA by a similar relatively simple mechanism (Li & Crothers, 1969; Dourlent & Hogrel, 1976; Ramstein et al., 1976; Marcandalli et al., 1984).

The interaction of anthracyclines with DNA is both generally slower and more complex than the interaction of phenanthridine and acridine intercalators with DNA. As can be seen in Figure 2, the SDS-driven dissociation of daunorubicin from DNA requires the sum of two exponentials for fitting of the results within experimental error. As indicated, these may represent two general families of rates for the 10 possible intercalation sites of DNA. Chaires et al. (1985) and Fox et al. (1985) have found similar biphasic results for the SDS-driven dissociation kinetics of the daunorubicin–DNA complex. There is a bigger difference between these two general rates of daunorubicin dissociation from DNA than in the single exponential dissociation rates for daunorubicin complexes with poly[d(G-C)]$_2$ and poly[d(A-T)]$_2$ (Figure 6). These results agree both qualitatively and quantitatively with those obtained for daunorubicin by Fox et al. (1985). Daunorubicin has significantly different interactions with alternating and nonalternating base pairs in DNA (Chaires, 1983), and the two classes of rate constants seen with duanorubicin dissociation from DNA may represent sequence-dependent, rather than base-pair-dependent, effects.

Mitoxantrone, ametantrone, and **4**, like daunorubicin, bind to DNA by intercalation (Lown et al., 1984, 1985). Mitoxantrone has a binding constant similar to that of daunorubicin and roughly 10 times larger than the binding constants for ametantrone and **4** (Lown et al., 1985). Like daunorubicin, **2**–**4** also exhibit biphasic dissociation kinetics from DNA complexes, and these probably also represent averages for groups of dissociation reactions. In agreement with binding results nLown et al., 1985), the overall dissociation of mitoxantrone from DNA is quite similar to that of daunorubicin in rate and considerably slower than those of ametantrone and **4** (Table I). Both dissociation rate constants are similar for DNA complexes with daunorubicin and mitoxantrone, but daunorubicin has a larger amplitude for the slower component. Ametantrone and **4** also have similar dissociation rate constants for both reaction phases, and the rates are 3–4 times faster than the rates for daunorubicin and mitoxantrone. Mitoxantrone and ametantrone have similar amplitudes for the two phases, but **4** has a larger amplitude for the fast phase and as a result has an apparent half-life that is only approximately half that of ametantrone and one-sixth that of mitoxantrone (Table I). The ratios of the fast to the slow rate constants for **1**–**4** are in the range **4**–**6**, suggesting that the compounds do not differ significantly in this respect.

Analysis of Figure 4 shows that the dissociation results of **4** from poly[d(A-T)]$_2$ and poly[d(G-C)]$_2$, like daunorubicin, can be fitted within experimental error by a single exponential function. The ametantrone results with these polymers can also be fitted with single-exponential curves. Unlike daunorubicin, however, ametantrone and **4** show pronounced base-pair dependence in their dissociation rate constants. The rate constants for dissociation of both from poly[d(A-T)]$_2$ are approximately 10 times larger than the dissociation rates from poly[d(G-C)]$_2$. At 20 °C the dissociation rate constants for daunorubicin and ametantrone from their poly[d(G-C)]$_2$ complexes are similar and approximately half that for the **4**–poly[d(G-C)]$_2$ complex. With poly[d(A-T)]$_2$ at 20 °C the dissociation constant for **4** is twice that for ametantrone, which is approximately seven times that for daunorubicin. When the polymer dissociation rate constants (Figure 6) are compared with those for DNA (Table I), it is seen that the dissociation rates of daunorubicin from the individual polymers fall between the two rates for DNA while those of ametantrone and **4** are similar to the two rates for DNA. The amplitudes for the DNA dissociations are different for ametantrone and **4**, however, indicating that there is no simple correlation between the DNA base-pair composition and the two rate processes. The simplification of the dissociation reactions for these compounds in moving from natural DNA to the synthetic polymers suggests that the complexity in their dissociation kinetics from DNA is due to a combination of base-pair- and sequence-dependent interactions, which are broken with different rates on dissociation from different sequences. With the uniform base-pair composition and sequence of the polymers, both the interactions and the dissociation reactions are, thus, simplified.

With the intercalators described above and even with complex molecules such as the antibiotics nogalamycin (Fox et al., 1985) and echinomycin (Fox et al., 1981), which require at least the sum of three exponential curves to fit their dissociation kinetics results with natural DNA samples, single-exponential reactions are obtained with the DNA polymers poly[d(A-T)]$_2$ and poly[d(G-C)]$_2$. As can be seen in Figure 5, however, mitoxantrone requires the sum of two exponential functions to fit the SDS-driven dissociation reactions from both poly[d(A-T)]$_2$ and poly[d(G-C)]$_2$. Mitoxantrone differs from ametantrone only by the presence of the two hydroxyl groups on the anthraquinone ring system (Figure 1). These hydroxyl groups result in an approximately 10-fold stronger binding of mitoxantrone to DNA relative to ametantrone (Lown et al., 1985) and a slower dissociation of mitoxantrone from DNA (Table I). It is not clear, however, why this would lead to more

complex polymer dissociation kinetics than with ametantrone, **4**, and daunorubicin, but there are two primary possibilities for this result: (i) mitoxantrone has significantly different possible DNA-binding modes, with both side chains in the same groove or with one side chain in each groove and/or (ii) mitoxantrone binds and dissociates differently with sites that are d(purine)-5′–3′-d(pyrimidine) vs. d(pyrimidine)-5′–3′-d-(purine). The first possibility has been investigated by Islam et al. (1985) and Balaji et al. (1985) using computer graphics and energy minimization techniques. Islam et al. (1985) concluded, on the basis of a specific dinucleotide intercalation geometry, that 1,4-substituted anthraquinones would bind more favorably to the double helix with both side chains in the major groove. An alternative model with one side chain in each groove was considered possible only with reoptimization of the dinucleotide intercalation geometry. The compounds that they investigated were, however, more analogous to **4** than to mitoxantrone. Balaji et al. (1985) investigated mitoxantrone and concluded that at least two binding modes were possible. The two rates observed with the polymer–mitoxantrone complexes could thus be due to the different types of intercalation complexes that mitoxantrone could favorably assume with any DNA sequence. Ametantrone and **4** should also be capable of forming both types of complex, but a single dissociation rate is observed for these compounds with the DNA polymers. The slowest dissociation of mitoxantrone would be expected to result from a complex with one side chain in each groove (Islam et al., 1985; Yen et al., 1982). With ametantrone and **4** the dissociation rates from the polymers are more similar to those for the faster dissociation process of mitoxantrone, suggesting that, if the model is correct, these compounds bind to DNA primarily with both side chains in one groove as predicted by Islam et al. (1985). In the complex with side chains in different grooves, the long axis of the anthraquinone ring system is approximately parallel to the base-pair long axes at the intercalation site. This model would then suggest that 5,8-$(OH)_2$ groups on the anthraquinone ring stabilize this type of structure and give mitoxantrone significant amounts of two distinct types of binding modes.

A second possibility for the polymer dissociation results is that mitoxantrone can bind to both purine–pyrimidine and pyrimidine–purine sequences in the polymers but has significantly different dissociation rate constants for these two types of sites. Ametantrone and **4** could be different either in binding to only one type of site or in binding to both types of sites but with similar dissociation rate constants for the sites.

Two-dimensional ^1H NMR studies (Lown et al., 1985) are in accord with intercalation of the mitoxantrone into d-$[CpGpCpG]_2$ in which the chromophore is aligned approximately perpendicular to the axis of the central base pair. More recent 2D ^1H and ^{31}P–^1H correlation NMR studies of the interaction of mitoxantrone with d$[CpGpApTpCpG]_2$ in H_2O indicate selective shifts of imino protons at the CpG sites. Moreover, maximal and selective shifts were observed with stoichiometries of drug:DNA of 1:1 and 2:1, corresponding to selective intercalation of the drug at the two CpG termini (Tong et al., 1985). This result is in accord wit the C·G base preference suggested by us earlier (Lown et al., 1985; Lown & Hanstock, 1985).

Chaires et al. (1985) have pointed out that the two observed SDS-driven dissociation rate constants for the daunorubicin–DNA complex could arise from two limiting mechanisms:

mechanism I

$$D + S \rightleftarrows C_1 \leftrightarrow C_2 \leftrightarrow C_3$$

mechanism II

$$D + S \rightleftharpoons C_1 \begin{matrix} \nearrow C_2 \\ \searrow C_3 \end{matrix}$$

C_1 is formed in a rapid bimolecular reaction and is identified as a weakly bound outside complex. Both C_2 and C_3 are formed either sequentially from C_1 as in mechanism I or independently from C_1 as in mechanism II. Both of these schemes fit the available results for the daunorubicin–DNA interaction and are difficult to distinguish (Chaires et al., 1985). Our analysis of the effect of ionic strength on the interaction of ethidium and propidium with DNA has shown that they bind with the simpler mechanism:

mechanism III

$$D + S \leftrightarrow C_1 \leftrightarrow C_2$$

where C_1 is also an outside or "condensed" preequilibrium bound form and C_2 is the intercalated state (Wilson et al., 1985). In this mechanism most of the sodium (or other nonspecific) counterion release from DNA on binding of cationic intercalators occurs on formation of the C_1 complex and much less in the transition from the condensed to the intercalated state. Mechanism II above involves two steps that are much like those for ethidium or propidium binding to DNA. The C_1 complex is rapidly formed and can then be converted to the intercalated C_2 or C_3. The rate differences from C_1 to C_2 or C_1 to C_3 could arise from specific base-pair, sequence, and/or conformational effects. The ionic strength dependence for binding through the C_1 state to either C_2 or C_3 should be very similar to that observed for the single complex in mechanism III. In mechanism I, however, the steps through C_1 to C_2 will have a salt dependence very much like the simple mechanism III, but the next step $C_2 \leftrightarrow C_3$ will be a conversion between states with very similar amounts of bound counterion and should have a very small ionic strength dependence. By monitoring the ionic strength dependence of the rate constants in a biphasic dissociation, it should then be possible to distinguish between mechanisms I and II. The ionic strength results for both dissociation rate constants for the daunorubicin–DNA complex was plotted in Figure 7. The predicted slope for dissociation of a monocation in mechanism III is 0.4 (Wilson et al., 1985) and both rate constants for a monocation like daunorubicin dissociating from DNA according to mechanism II should also have a slope of 0.4. That is the result observed in Figure 7, suggesting that mechanism II represents the correct mechanism for the biphasic dissociation of daunorubicin from DNA. As can also be seen in Figure 7, mitoxantrone, too, has very similar slopes for both steps in its biphasic SDS-driven dissociation from DNA. Each slope is in good agreement with the observed slope for monophasic dissociation of the dication propidium from DNA and with theoretical predictions (Wilson et al., 1985). These results suggest that mechanism II also represents the mechanism for the interaction of mitoxantrone type dications with DNA. It will be of interest to investigate the ionic strength dependence of the dissociation kinetics for other molecules that bind to DNA with complex kinetics to determine the generality of this mechanism.

Finally, it should be pointed out that mitoxantrone and daunorubicin, both of which have shown excellent anticancer activity, bind strongly to DNA under physiological conditions and have slower dissociation kinetics from their DNA com-

plexes than phenanthridine, acridine, and other similar intercalators. The suggestion by Müller and Crothers (1968) that slow dissociation kinetics may be essential for activity of these types of compounds is supported by these results, and it would seem that kinetics analysis could be a useful physical method in evaluating new potential intercalators for possible antitumor activity. It should be noted, however, that none of these intercalators have the very slow dissociation rates observed for actinomycin complexes (Müller & Crothers, 1968). These results do not exclude the possibility of the contribution of alternative pathways, perhaps mediated enzymatically, to the overall toxicity of these clinically useful agents.

ACKNOWLEDGMENTS

We thank Drs. W. A. Denny, L. P. G. Wakelin, S. Neidle, and G. Kotovych for helpful discussions and Drs. Denny and Wakelin for a preprint of their manuscript on anthraquinone intercalator kinetics. We also thank Dr. K. C. Murdock of Lederle Laboratories of the American Cyanamid Co. for generously supplying the compounds used in this research.

Registry No. **1**, 20830-81-3; **1**·2poly[d(G-C)], 103883-63-2; **1**·2poly[d(A-T)], 103883-64-3; **2**, 65271-80-9; **2**·2poly[d(G-C)], 103883-62-1; **3**, 64862-96-0; **3**·2poly[d(G-C)], 103883-65-4; **3**·2poly[d(A-T)], 103883-66-5; **4**, 69895-68-7; **4**·2poly[d(G-C)], 103883-67-6; **4**·2poly[d(A-T)], 103883-68-7.

REFERENCES

Balaji, V. N., Dixon, J. S., Smith, D. H., Venkataragavan, R., & Murdock, K. C. (1985) *Ann. N.Y. Acad. Sci. 439*, 140–161.

Chaires, J. B. (1983) *Biochemistry 22*, 4204–4211.

Chaires, J. B., Dattagupta, N., & Crothers, D. M. (1985) *Biochemistry 24*, 260–267.

Chandrasekaran, S., Krishnamoorthy, C. R., Jones, R. L., Smith, J. C., & Wilson, W. D. (1984) *Biochem. Biophys. Res. Commun. 122*, 804–809.

Citarella, R. V., Wallace, R. E., Murdock, K. C., Angier, R. B., Dun, F. E., & Forbes, M. (1982) *Cancer Res. 42*, 440–444.

Dourlent, M., & Hogrel, J. F. (1976) *Biochemistry 15*, 430–436.

Fox, K. R., & Waring, M. J. (1984) *Eur. J. Biochem. 145*, 579–586.

Fox, K. R., Wakelin, L. P. G., & Waring, M. J. (1981) *Biochemistry 20*, 5768–5779.

Fox, K. R., Brassett, C., & Waring, M. J. (1985) *Biochim. Biophys. Acta 840*, 383–392.

Islam, S. A., Neidle, S., Gandecha, B. M., Partridge, M., Patterson, L. H., & Brown, J. R. (1985) *J. Med. Chem. 28*, 857–864.

Jovin, T., & Striker, G. (1977) in *Chemical Relaxation in Molecular Biology* (Pecht, I., & Rigler, R., Eds.) pp 245–281, Springer-Verlag, New York.

Li, H. J., & Crothers, D. M. (1969) *J. Mol. Biol. 39*, 461–477.

Lown, J. W., & Hanstock, C. C. (1985) *J. Biomol. Struct. Dyn. 2*, 1097–1106.

Lown, J. W., Hanstock, C. C., Bradley, R. D., & Scraba, D. G. (1984) *Mol. Pharmacol. 25*, 178–184.

Lown, J. W., Morgan, A. R., Yen, S. F., Wang, Y. H., & Wilson, W. D. (1985) *Biochemistry 24*, 4028–4035.

Macgregor, R. B., Clegg, R. M., & Jovin, T. M. (1985) *Biochemistry 24*, 5503–5510.

Mandal, C., Englander, S. W., & Kallenbach, N. R. (1980) *Biochemistry 19*, 5819–5825.

Marcandalli, B., Winzek, C., & Holzwarth, J. F. (1984) *Ber. Bunsen-Ges. Phys. Chem. 88*, 368–374.

Müller, W., & Crothers, D. M. (1968) *J. Mol. Biol. 35*, 251–290.

Murdock, K. C., Child, R., Fabio, P. F., Angier, R. B., Wallace, R. E., Dun, F. E., & Citarella, R. V. (1979) *J. Med. Chem. 22*, 1024–1034.

Ramstein, J., Ehrenberg, M., & Rigler, R. (1980) *Biochemistry 19*, 3938–3948.

Rozencweig, M., von Hoff, D. D., & Staquet, M. J., Eds. (1983) *New Anticancer Drugs: Mitoxantrone and Bisantrene*, Vol. 12, Raven, New York.

Ryan, D. P., & Crothers, D. M. (1984) *Biopolymers 23*, 537–562.

Shafer, R. H., Burnette, R. R., & Mirau, P. A. (1980) *Nucleic Acids Res. 8*, 1121–1132.

Tong, J. P. K., Lown, J. W., & Kotovych, G. (1986) *Biochemistry* (submitted for publication).

Turner, B. W., Pettigrew, D. W., & Ackers, G. K. (1981) *Methods Enzymol. 71*, 596–628.

Waring, M. J. (1981) in *The Molecular Basis of Antibiotic Action* (Gale, E. F., Cundliffe, E., Reynolds, P. E., Richmond, M. H., & Waring, M. J., Eds.) 2nd ed., p 287, Wiley, New York.

Wilson, W. D., Grier, D., Reimer, R., Bauman, J. D., Preston, J. F., & Gabbay, E. J. (1976) *J. Med. Chem. 19*, 381–384.

Wilson, W. D., Krishnamoorthy, C. R., & Wang, Y. H. (1985) *Biopolymers 24*, 1941–1961.

Yen, S. F., Gabbay, E. J., & Wilson, W. D. (1982) *Biochemistry 21*, 2070–2076.